Gadolinium enhancement of cranial nerves: implications for interstitial fluid drainage from brainstem into cranial nerves in man

Aravinthan Varatharaj[1,2], Roxana O Carare[1], Roy O Weller[1], Mary Gawne-Cain[2], Ian Galea[1,2]

[1] Clinical Neurosciences, Clinical and Experimental Sciences, Faculty of Medicine, University of Southampton, Southampton, UK

[2] Wessex Neurological Centre, University Hospital Southampton NHS Foundation Trust, Southampton, UK

Corresponding author: Professor Ian Galea, Clinical Neurosciences, Clinical and Experimental Sciences, Faculty of Medicine, University of Southampton, Tremona Road, Southampton, SO16 6YD, UK

I.Galea@soton.ac.uk

Competing Interest Statement

None

Keywords

interstitial fluid drainage; gadolinium; trigeminal nerve; contrast-enhanced magnetic resonance imaging

Abstract

Drainage of interstitial fluid and solutes from the brainstem has not been well studied. To map one drainage pathway in the human brainstem, we took advantage of the focal blood-brain barrier disruption occurring in a multiple sclerosis brainstem lesion, coupled with intravenous injection of gadolinium, which simulates an intraparenchymal injection of gadolinium tracer within the restricted confines of this small brain region. Using high-resolution magnetic resonance imaging we show how it is possible for interstitial fluid to drain into the adjacent trigeminal and oculomotor nerves, in keeping with a pathway of communication between the extracellular spaces of the brainstem and cranial nerve parenchyma.

Introduction

Normally, interstitial fluid (ISF) and soluble metabolites are eliminated from brain tissue by diffusion through the extracellular spaces and then by rapid drainage along the walls of capillaries and arteries to lymph nodes, the Intramural Peri-Arterial Drainage (IPAD) pathway (1). Cerebrospinal fluid drains into the arachnoid villi, meningeal lymphatics and along channels adjacent to olfactory nerves but there is little evidence for connections between these structures and the anatomical pathways for the drainage of ISF from the brain (2). The glymphatic hypothesis states that ISF drains along the walls of veins but this is controversial and evidence from human pathological studies of cerebral amyloid angiopathy (occurring mainly in the walls of arteries and very rarely in veins) argues against the drainage of ISF along the walls of veins (3, 4).

Drainage of ISF and solutes from the brainstem has not been well studied. To map this drainage pathway in the human brainstem, we took advantage of the focal blood-brain barrier (BBB) disruption occurring in a multiple sclerosis (MS) brainstem lesion, coupled with intravenous injection of gadolinium, which simulates an intraparenchymal injection of gadolinium tracer within the restricted confines of this small brain region. We used high-resolution contrast-enhanced MRI to track the subsequent distribution of gadolinium in the adjacent cranial nerves.

Results

Images were acquired before intravenous injection of gadolinium-based contrast, and serially for 49 minutes in a 37-year-old man with a visibly-enhancing pontine MS lesion, and a healthy 38-year-old man. The MS lesion was located in the left pons (Figure 1A) and enhanced visibly after contrast (Figure 1B-C). The lesion was not associated with any appreciable swelling, the normal pontine contour was preserved and the area of high T2-

weighted signal (Figure 2D) did not extend beyond the borders of the lesion as indicated by T1-weighted hypointensity (Figure 1A). Visible contrast enhancement was observed in the trigeminal (Figure 1D-F), oculomotor (Figure 1G-I), vagus and glossopharyngeal nerves (Figure 1M-O), but not in the facial and vestibulocochlear nerves (Figure 1J-L). The enhancement was greater on the ipsilateral side.

Quantitative analysis of signal intensity was performed, normalising to pre-contrast signal. The pontine MS lesion showed rapid initial enhancement which progressively slowed, consistent with an exponential plateau pattern (Figure 2A). Regions of interest were first placed over the trigeminal nerves as they are of larger diameter compared to the other cranial nerves (Figure 2A). The ipsilateral trigeminal nerve enhanced with a temporal profile similar to that of the MS lesion, but with reduced intensity (Figure 2A). Contrast was present in the contralateral trigeminal nerve, though here the signal was dampened further (Figure 2A). Contrast present in the perilesional normal-appearing tissue could be differentiated from normal-appearing pontine tissue distant from the lesion (Figure 2A).

There were two possible sources for the trigeminal nerve enhancement: (i) contrast diffusing down the trigeminal nerve from the brainstem and (ii) contrast derived from the blood supply to the nerve trunk. In order to distinguish between these two sources, we took advantage of the microanatomy of the trigeminal nerve. The first 4mm of the nerve most proximal to the brainstem, referred to as the "central" portion of the nerve (5) (since it retains histological characteristics of CNS tissue) is devoid of perineurium and epineurium. On the other hand the rest of the cranial nerve, referred to as the "peripheral" portion, has a perineurium and epineurium, which are vascularized and lack a blood-nerve barrier (6). Dividing the nerve into "central" and "peripheral" segments, the kinetics of enhancement were significantly different between the two (Figure 2B), confirmed by a mixed ANOVA with repeated measures ($p < 10^{-6}$, $F(1,201) = 27.4$ for segment). The timing of enhancement in the

peripheral segment was earlier and larger in magnitude. On the other hand, the timing of the proximal segment mirrored that of the perilesional normal-appearing brain tissue, in keeping with continuity of ISF between the brainstem tissue and the trigeminal nerve endoneurium.

Regions of interest were placed over the oculomotor, facial, vestibulocochlear, and glossopharyngeal/vagus nerves. These nerves have a small diameter approaching the limit of resolution of MRI, so partial volume effects are likely. Since no increase in signal was measured in the cerebrospinal fluid (Figure 2C), inclusion of surrounding cerebrospinal fluid within the measured voxels would be expected to reduce the measured signal intensity. Despite this, there was still evidence of enhancement (Figure 2C), with the exception of the vestibulocochlear nerve. It was not possible to accurately identify and/or quantitate the trochlear, abducens, accessory, and hypoglossal nerves, due to their small size and/or tortuousity and the resolution limit ($1mm^3$). No cranial nerve enhancement was observed in the control individual (Figure 2E).

Discussion

Lesion enhancement was consistent with BBB breakdown delivering gadolinium contrast directly into the brainstem ISF, which then appeared within the cranial nerves. The timing and magnitude of the signal intensity within the central portion of the trigeminal nerve was similar to that of the normal-appearing tissue interposed between the lesion and the nerve, indicative of continuity of ISF spaces in the two compartments. The central portion of the trigeminal nerve is devoid of perineurium and endoneurium, which contributed to contrast enhancement in the distal nerve. Cranial nerves or their root entry zones were not inflamed, since no T2 signal abnormality was present in these areas.

Recent studies have suggested the presence of cells with lymphatic markers in cranial nerves (7, 8) but there are no lymphatic vessels in normal cranial or peripheral nerves (9) and

drainage routes within nerves have yet to be clearly defined. With the presence of blood-nerve and perineurial barriers (10), it is possible that drainage in cranial nerves is similar to the brain, i.e. along the walls of capillaries and arteries (1). Similarly, we propose that there is continuity between the basement membranes of capillaries in the brainstem (IPAD pathway) and trigeminal nerve endoneurium.

We were careful to select a MS lesion which was not visibly oedematous, to minimize the likelihood that high local interstitial pressure opens up alternative pathways for ISF drainage. Nevertheless, the fact remains that we relied on MS pathology, to deliver a high dose of gadolinium tracer into the brainstem parenchyma. Local inflammation would increase permeability of blood vessel walls. Structural changes to the IPAD pathway occur during MS such as basement membrane damage secondary to matrix metalloproteinases (11), but whether ISF drainage is unchanged, increased or decreased remains to be shown.

The drainage pathway of interstitial solutes from the brain along cranial nerves is of clinical importance. It may play a role in migraine, enabling calcitonin gene-related peptide (CGRP) released from the trigeminal nuclei within the brainstem to reach CGRP receptors in meningeal arteries to trigger vasodilatation (12). The same conduit may allow transport of intranasal therapeutics into the brainstem (13). The pathway of communication between the extracellular spaces of the brain and nerve needs further study.

Materials and Methods

The study protocol had institutional (University of Southampton Research Ethics Committee reference ERGO 46018) and national Health Research Authority (reference 18/LO/2015) approvals. Written informed consent including publication of images was obtained after the patients had time to read information about the study and ask any questions, as per approved protocol. Full methods are in the *SI Appendix*. In brief, imaging was performed on a 3T MR

unit (Skyra, Siemens, Erlangen, Germany) using a 20-element phased-array head and neck coil. 3D MP-RAGE images covering the whole brain were acquired before contrast injection (Gd-DO3A-butrol; Bayer; Newbury, UK) (0 minutes), and at 7, 14, 21, 28, 35, and 49 minutes thereafter (1.0 mm^3). Additional pre-contrast sequences were axial turbo-spin echo T2-weighted and 3D FLAIR. MPRAGE images were affine-registered and read into MATLAB (Mathworks, Natick, USA). Signal values at each timepoint were converted to enhancement indices by normalising to pre-contrast signal. Regions of interest (ROIs) were drawn manually and the mean value within each ROI over time was calculated.

Data availability

Anonymized source images are available from the University of Southampton's research repository at https://doi.org/10.5258/SOTON/D1824

Acknowledgements

We thank Chris Everitt, radiographer at University Hospital Southampton NHS Foundation Trust. The study was funded by the Medical Research Council (MR/R017352/1).

References

1. Carare RO, *et al.* (2020) Clearance of interstitial fluid (ISF) and CSF (CLIC) group—part of Vascular Professional Interest Area (PIA). *Alzheimer's & Dementia: Diagnosis, Assessment & Disease Monitoring* 12(1):e12053.
2. Engelhardt B, *et al.* (2016) Vascular, glial, and lymphatic immune gateways of the central nervous system. *Acta neuropathologica* 132(3):317-338.
3. Keable A, *et al.* (2016) Deposition of amyloid beta in the walls of human leptomeningeal arteries in relation to perivascular drainage pathways in cerebral amyloid angiopathy. *Biochimica et biophysica acta* 1862(5):1037-1046.
4. Carare RO, Hawkes CA, Jeffrey M, Kalaria RN, & Weller RO (2013) Review: cerebral amyloid angiopathy, prion angiopathy, CADASIL and the spectrum of protein elimination failure angiopathies (PEFA) in neurodegenerative disease with a focus on therapy. *Neuropathology and applied neurobiology* 39(6):593-611.
5. Guclu B, *et al.* (2011) Cranial nerve vascular compression syndromes of the trigeminal, facial and vago-glossopharyngeal nerves: comparative anatomical study of the central myelin portion and transitional zone; correlations with incidences of corresponding hyperactive dysfunctional syndromes. *Acta Neurochirurgica* 153(12):2365-2375.
6. Olsson Y (1968) Topographical differences in the vascular permeability of the peripheral nervous system. *Acta Neuropathologica* 10(1):26-33.
7. Aspelund A, *et al.* (2015) A dural lymphatic vascular system that drains brain interstitial fluid and macromolecules. *Journal of Experimental Medicine* 212(7):991-999.

8. Ma Q, Ineichen BV, Detmar M, & Proulx ST (2017) Outflow of cerebrospinal fluid is predominantly through lymphatic vessels and is reduced in aged mice. *Nat Commun* 8(1):1434.

9. Meng F-W, Jing X-N, Song G-H, Jie L-L, & Shen F-F (2020) Prox1 induces new lymphatic vessel formation and promotes nerve reconstruction in a mouse model of sciatic nerve crush injury. *Journal of Anatomy* 237(5):933-940.

10. Ahmed AM & Weller RO (1979) The blood-nerve barrier and reconstitution of the perineurium following nerve grafting. *Neuropathology and Applied Neurobiology* 5(6):469-483.

11. Agrawal S, *et al.* (2006) Dystroglycan is selectively cleaved at the parenchymal basement membrane at sites of leukocyte extravasation in experimental autoimmune encephalomyelitis. *Journal of Experimental Medicine* 203(4):1007-1019.

12. Messlinger K (2018) The big CGRP flood - sources, sinks and signalling sites in the trigeminovascular system. *J Headache Pain* 19(1):22.

13. Thorne RG, Pronk GJ, Padmanabhan V, & Frey WH, 2nd (2004) Delivery of insulin-like growth factor-I to the rat brain and spinal cord along olfactory and trigeminal pathways following intranasal administration. *Neuroscience* 127(2):481-496.

Figures

Fig. 1. The evolution of contrast enhancement on T1-weighted images at early (7 minutes) and late (49 minutes) stages, for the pontine lesion (*A-C*), and ipsilateral trigeminal (*D-F*), oculomotor (*G-I*), facial and vestibulocochlear (*J-L*), and vagus and glossopharyngeal nerves (*M-O*).

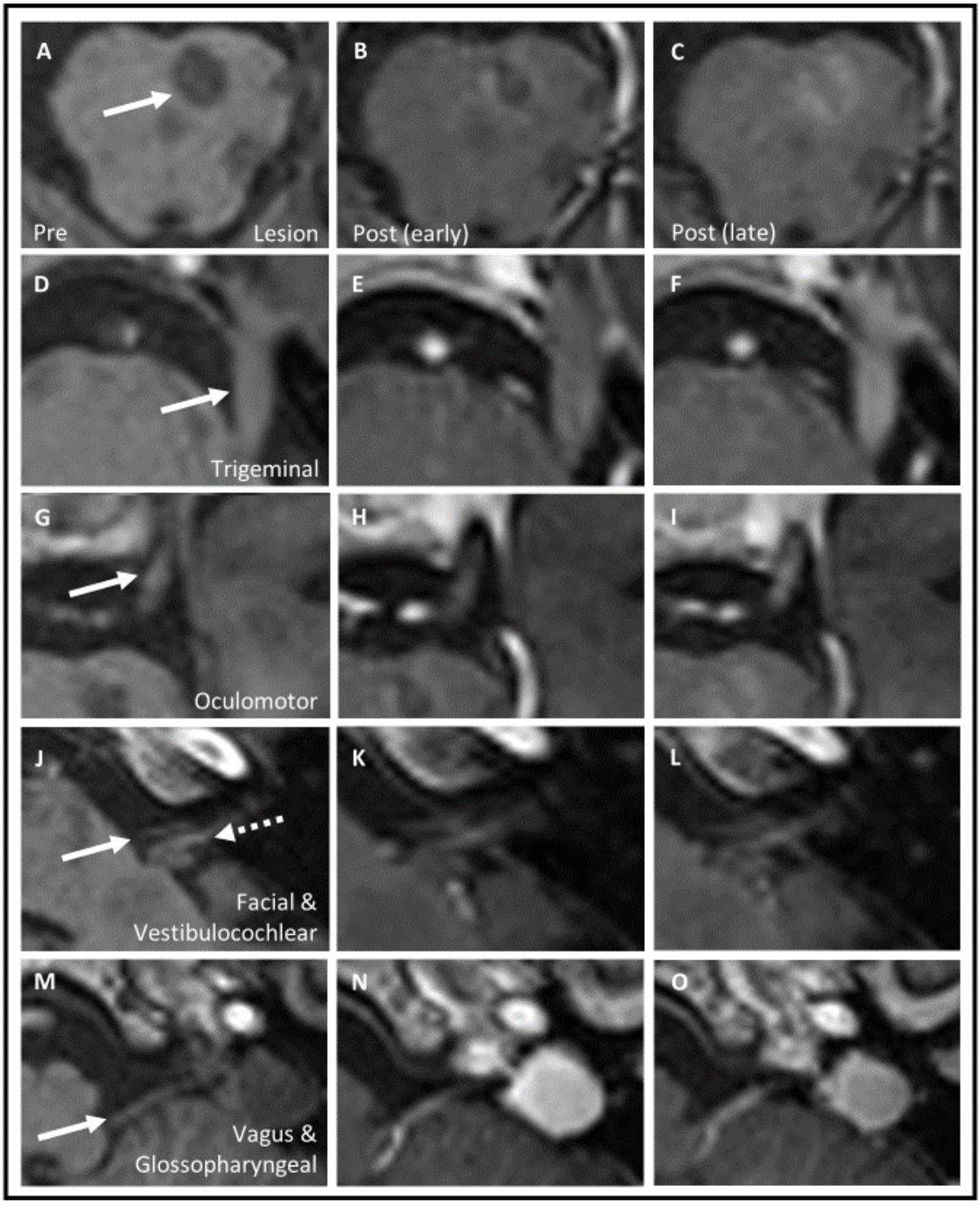

Fig. 2. *(A)* Temporal profiles of enhancement for the pontine lesion, peri-lesional normal-appearing pontine tissue, distant pontine normal-appearing tissue, and both trigeminal nerves. The quantified regions-of-interest (ROIs) are colour-matched. *(B)* Temporal profiles of enhancement for the ipsilateral trigeminal nerve, divided into the proximal 4mm ("central segment") and the remainder of the distal nerve ("peripheral segment"). The profile for peri-lesional pontine tissue is overlaid for comparison. *(C)* Temporal profiles of enhancement and locations of ROIs for the ipsilateral oculomotor, facial, vestibulocochlear, vagus and glossopharyngeal nerves, and cerebrospinal fluid (CSF) in the prepontine cistern. Note that these nerves and therefore ROIs are significantly smaller than those in Figure 2A, and consequently the temporal profiles are noisier. *(D)* Axial slices at the level of the superior pons with the lesion (arrows) visible on T2-weighted, and FLAIR (fluid-attenuated inversion recovery) sequences. *(E)* Absence of contrast enhancement on T1-weighted images in the trigeminal nerves of the control individual. This individual did not tolerate the full protocol and so the last timepoint is 28 minutes post-contrast.

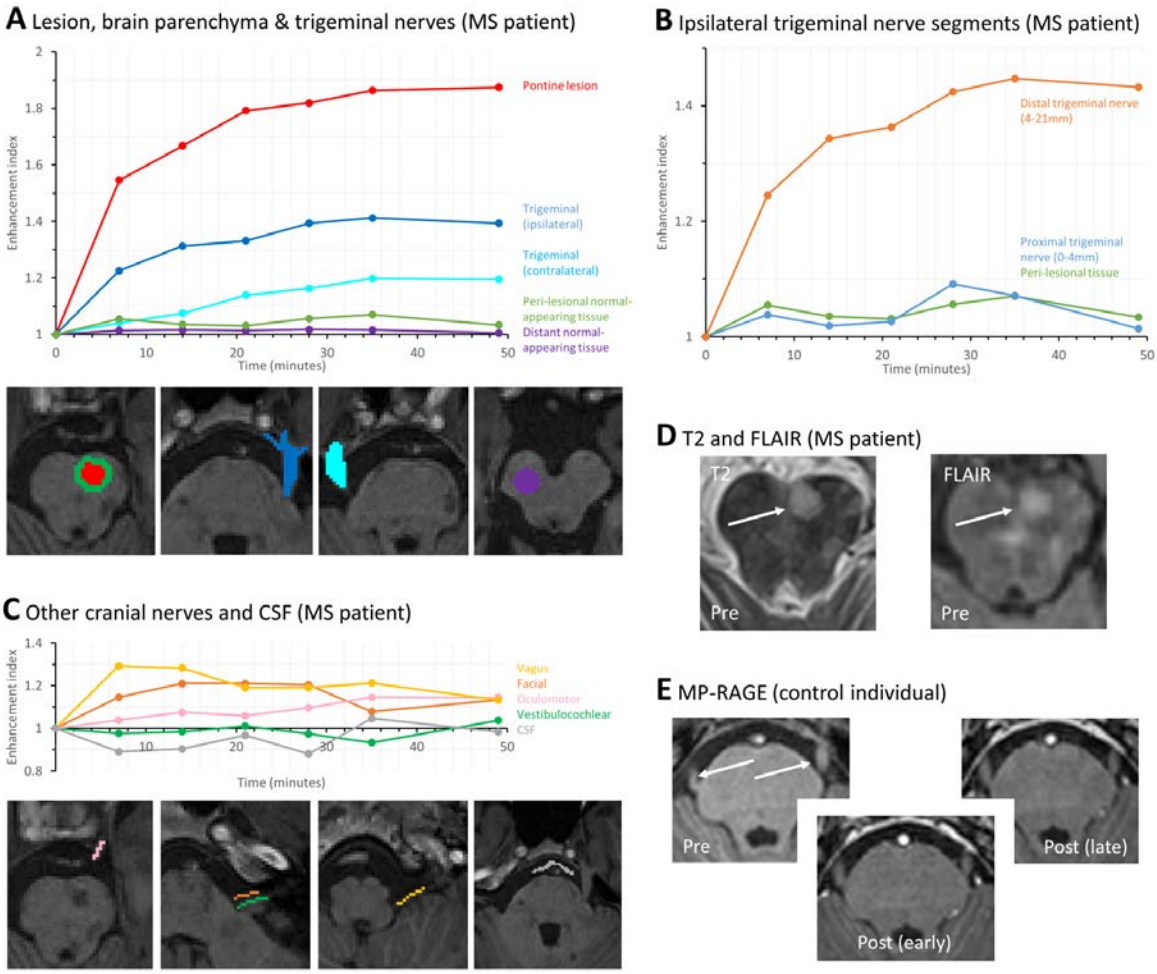

PNAS
www.pnas.org

Supplementary Information for

Gadolinium enhancement of cranial nerves: implications for interstitial fluid drainage from brainstem into cranial nerves in man

Aravinthan Varatharaj[1,2], Roxana O Carare[1], Roy O Weller[1], Mary Gawne-Cain[2], Ian Galea[1,2]

[1] Clinical Neurosciences, Clinical and Experimental Sciences, Faculty of Medicine, University of Southampton, Southampton, UK
[2] Wessex Neurological Centre, University Hospital Southampton NHS Foundation Trust, Southampton, UK

Corresponding author: Professor Ian Galea, Clinical Neurosciences, Clinical and Experimental Sciences, Faculty of Medicine, University of Southampton, Tremona Road, Southampton, SO16 6YD, UK
I.Galea@soton.ac.uk

This PDF file includes:

Supplementary text (Materials and Methods)

Materials and Methods

The study protocol had institutional (University of Southampton Research Ethics Committee reference ERGO 46018) and national Health Research Authority (reference 18/LO/2015) approvals. Written informed consent including publication of images was obtained after the patients had time to read information about the study and ask any questions, as per approved protocol. Imaging was performed on a 3T MR unit (Skyra, Siemens, Erlangen, Germany) at University Hospital Southampton NHS Foundation Trust, using a 20-element phased-array head and neck coil. 3D magnetization prepared-rapid gradient echo (MP-RAGE) images covering the whole brain were acquired before the injection of contrast (0 minutes), and at 7, 14, 21, 28, 35, and 49 minutes thereafter (TR = 2200 ms, TE = 2.45 ms, TI = 900 ms, flip angle = 8°, parallel imaging factor =2, field-of-view 250 × 250 × 176 mm^3, voxel size 1.0 × 1.0 × 1.0 mm^3). The contrast agent was Gadovist (Gd-DO3A-butrol, Gadobutrol; Bayer; Newbury, UK), chosen due to high relaxivity (1), injected intravenously at a rate of 2-4 ml/s in a double half-dose injection scheme, with 0.05 mmol kg^{-1} given 2 minutes apart (2). Additional pre-contrast sequences were axial turbo spin echo T2-weighted (TR = 4400 ms, TE = 9/90 ms, field-of-view 250 × 203 ×149 mm^3, voxel size 1.0 × 1.0 × 3.0 mm^3, 45 slices, distance factor = 10%) and 3D fluid-attenuated inversion recovery (TR = 5000 ms, TE = 397 ms, TI = 1800 ms, field-of-view = 256 × 248 x 194 mm^3, voxel size 1.0 x 1.0 x 1.1 mm^3, 176 slices). All MPRAGE images were affine-registered using FSL-FLIRT (3) to correct for subject motion, and read into MATLAB (Mathworks, Natick, USA). Signal values at each timepoint were converted to enhancement indices by normalising to pre-contrast signal (index values above 1 indicate signal enhancement due to the presence of contrast

agent). Regions of interest (ROIs) were drawn manually and the temporal kinetics of enhancement extracted as the mean value within each ROI over time. For ROIs in normal-appearing brain tissue, the possible encroachment of T1-isointense lesion voxels was prevented by subtracting the FLAIR-derived lesion mask.

SI References

1. Shen Y, *et al.* (2015) T1 relaxivities of gadolinium-based magnetic resonance contrast agents in human whole blood at 1.5, 3, and 7 T. *Invest Radiol* 50(5):330-338.
2. Larsson HB, Courivaud F, Rostrup E, & Hansen AE (2009) Measurement of brain perfusion, blood volume, and blood-brain barrier permeability, using dynamic contrast-enhanced T(1)-weighted MRI at 3 tesla. *Magn Reson Med* 62(5):1270-1281.
3. Jenkinson M, Bannister P, Brady M, & Smith S (2002) Improved optimization for the robust and accurate linear registration and motion correction of brain images. *Neuroimage* 17(2):825-841.